ICIC Express Letters
Volume **10**, Number **11**, November **2016**

ICIC International ©2016 ISSN 1881-803X
pp. **2773–2778**

FINITE DIFFERENCE METHOD FOR ELECTRO-OSMOTIC FLOW AND ITS CONVERGENCE

Pearanat Chuchard[1], Masaaki Tamagawa[2] and Somsak Orankitjaroen[1]

[1]Department of Mathematics
Faculty of Science
Mahidol University
Rama VI Road, Ratchathewi District, Bangkok 10400, Thailand
pearanat.chu@student.mahidol.ac.th; somsak.ora@mahidol.ac.th

[2]Department of Biological Functions Engineering
Graduate School of Life Science and Systems Engineering
Kyushu Institute of Technology
Hibikino 2-4, Wakamatsu-ku, Kitakyushu, Fukuoka 808-0196, Japan
tama@life.kyutech.ac.jp

Received April 2016; accepted July 2016

Abstract. *Electro-osmotic flow through a cylindrical tube is investigated numerically based on the finite difference method with the successive over relaxation (SOR) method using the Fortran language. The effect of the pressure weight parameter β and the tolerance τ of the SOR method on the SOR convergent rate and the maximum error of the continuity equation are examined. The results show that a low-value of β and a high-value of τ give a good convergent rate of the SOR method. Moreover, the value of the external electric field plays an important role on the convergent rate of the SOR method but it has no impact on the maximum error of the continuity equation.*
Keywords: Electro-osmosis, Electro-osmotic flow, Finite difference method, Convergence

1. **Introduction.** Over the last decade, microfluidics has been widely developed for the applications, for example, lab on a chip, DNA chip, and micro-mixer system [1-3]. Due to the micro-scale of the channel in microfluidics, the electro-osmotic force plays an important role and will become a powerful tool to control the fluid phenomena [4]. Therefore, one of the key to success in the microfluidics advance, especially in a system design, is the understanding in the behavior of the electro-osmotic flow (EOF) [5-7]. To investigate the phenomena of EOF, the finite difference method (FDM) is one of the well-known methods giving a good accurate numerical result and fast convergence. Recently, there are a number of researches involving FDM on EOF. Aboelkassem [8] presented the numerical simulation of electro-osmotic flow patterns using FDM. Their governing equations are simplified by eliminating transient and convection terms in momentum equations. Li et al. [9] and Reshadi et al. [10] also investigated the behavior of electro-osmotic flow in microchannel using FDM. The pressure gradient term, in their works, on the Navier-Stokes equations is ignored or assumed to be a constant. Although the simplification of the governing equations is a general methodology in computational fluid dynamics, this may result in an unrealistic behavior in certain circumstances when the eliminated term has a significant value. Moreover, all works mentioned above do not propose the efficiency of the method and the effect of the involved parameters.

In this paper, we propose the mathematical model of EOF induced by acceleration, convection, pressure, viscosity and external electric field on an electrolyte fluid through a cylindrical microchannel. The flow behavior is simulated using FDM and successive over relaxation (SOR) method on the incompressible Navier-Stokes equations coupled with

the electroosmotic body force expressed as the Debye-Huckle linear approximation. The effects of the pressure weight parameter and the SOR tolerance on the convergent rate and the error of the continuity equation are investigated to obtain the efficient algorithm. In addition, the influence of applied external electric field is determined. The introduction is presented in Section 1. The governing equations and the computational models are given in Section 2. The main results with the discussions and the conclusions are shown in Sections 3 and 4, respectively.

2. Governing Equations and Computational Models.

2.1. Governing equations.

Assuming an axisymmetric flow around the z-axis, we express the dimensionless fundamental equations of the transient incompressible electro-osmotic flow through a cylindrical tube in a cylindrical coordinate system (r, ϕ, z) as:

$$\frac{1}{\tilde{r}}\frac{\partial(\tilde{r}\tilde{u}_r)}{\partial\tilde{r}} + \frac{\partial\tilde{u}_z}{\partial\tilde{z}} = 0 \tag{1}$$

$$\frac{\partial\tilde{u}_r}{\partial\tilde{t}} + \tilde{u}_r\frac{\partial\tilde{u}_r}{\partial\tilde{r}} + \tilde{u}_z\frac{\partial\tilde{u}_r}{\partial\tilde{z}} = \frac{1}{Re}\left[-\frac{\partial\tilde{p}}{\partial\tilde{r}} + \frac{1}{\tilde{r}}\frac{\partial}{\partial\tilde{r}}\left(\tilde{r}\frac{\partial\tilde{u}_r}{\partial\tilde{r}}\right) + \frac{\partial^2\tilde{u}_r}{\partial\tilde{z}^2} - \frac{\tilde{u}_r}{\tilde{r}^2}\right] \tag{2}$$

$$\frac{\partial\tilde{u}_z}{\partial\tilde{t}} + \tilde{u}_r\frac{\partial\tilde{u}_z}{\partial\tilde{r}} + \tilde{u}_z\frac{\partial\tilde{u}_z}{\partial\tilde{z}} = \frac{1}{Re}\left[-\frac{\partial\tilde{p}}{\partial\tilde{z}} + \frac{1}{\tilde{r}}\frac{\partial}{\partial\tilde{r}}\left(\tilde{r}\frac{\partial\tilde{u}_z}{\partial\tilde{r}}\right) + \frac{\partial^2\tilde{u}_z}{\partial\tilde{z}^2} - \frac{\varepsilon\tilde{E}}{\tilde{r}}\frac{\partial}{\partial\tilde{r}}\left(\tilde{r}\frac{\partial\tilde{\Psi}}{\partial\tilde{r}}\right)\right] \tag{3}$$

$$\frac{1}{\tilde{r}}\frac{\partial}{\partial\tilde{r}}\left(\tilde{r}\frac{\partial\tilde{\Psi}}{\partial\tilde{r}}\right) - \frac{1}{\tilde{\lambda}_D^2}\tilde{\Psi} = 0 \tag{4}$$

Here u_r and u_z are the fluid velocity in r- and z-direction, p is the fluid pressure, Ψ is the potential distribution inside the tube, E is the external electric field, E_{ref} is the chosen referenced value of electric field, R is the radius of channel cross-section (see Figure 1(a)), and ρ, μ, ε, ζ, and λ_D are the fluid properties shown in Table 1; the dimensionless variables are defined as: $\tilde{r} = r/R$, $\tilde{z} = z/R$, $V_{EOF} = \varepsilon\zeta E_{ref}/\mu$, $\tilde{u}_r = u/V_{EOF}$, $\tilde{u}_z = u_z/V_{EOF}$, $\tilde{p} = p/(\varepsilon\zeta E_{ref}/R)$, $\tilde{\Psi} = \Psi/\zeta$, $\tilde{E} = E/E_{ref}$, $\tilde{\lambda}_D = \lambda_D/R$, $\tilde{t} = t/(R/V_{EOF})$, $Re = \rho R V_{EOF}/\mu$. Equation (1) is known as the continuity equation, while Equations (2) and (3) are the incompressible Navier-Stokes equations with electro-osmotic force. In case of a low-value of potential inside the tube (less than 25 mV), $\tilde{\Psi}$ can be expressed by the Debye-Huckle linear approximation as shown in Equation (4).

We, in this study, consider electro-osmotic flow through a cylindrical tube as shown in Figure 1(a). The computational domain is in 2 dimensions (ϕ-direction is vanished by the symmetric property of the flow around the z-axis) and is demonstrated in Figure 1(b) with the dimensionless radius $\tilde{R} = 1$ and the dimensionless length $\tilde{l} = 5$. Fluid is assumed to be an aqueous KCl solution (1 : 1 electrolytes) with $Re = 1.6 \times 10^{-3}$ and its properties are presented in Table 1. The referenced external electric field E_{ref} is set at 500 Vm^{-1}.

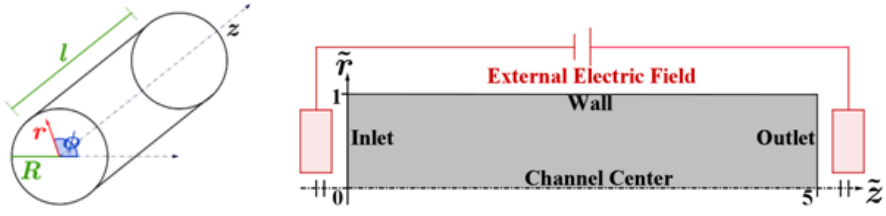

(a) (b)

FIGURE 1. (a) The cylindrical tube, and (b) the 2-dimensional computational domain

Table 1. Fluid properties [4]

Parameters	Symbol	Value	Unit
Fluid density	ρ	1.00×10^{3}	kgm^{-3}
Fluid viscosity	μ	0.90×10^{-3}	$\mathrm{kgm}^{-1}\mathrm{s}^{-1}$
Fluid permittivity	ε	6.95×10^{-10}	$\mathrm{CV}^{-1}\mathrm{m}^{-1}$
Zeta potential	ζ	2.49×10^{-2}	V
Electrical double layer thickness	λ_D	2.50×10^{-5}	m

The boundary conditions are given by: 1) Inlet: $\tilde{u}_r = 0$ and $\tilde{u}_z = 1.04$; 2) Outlet: $\tilde{p} = 0$; 3) Channel center: $\tilde{u}_r = 0$ and $\tilde{\Psi} = 0$; 4) Wall: no slip and $\tilde{\Psi} = 1$.

2.2. **Computational models.** By computing Equations (2) to (4) using FDM, now we can update the value of next time step of the dimensionless fluid velocity $\tilde{u}_r^{k+1}$ and $\tilde{u}_z^{k+1}$. However, in general, $\tilde{u}_r^{k+1}$ and $\tilde{u}_z^{k+1}$ do not satisfy the continuity equation (1). Moreover, there is no computation for updating the fluid pressure $\tilde{p}^{k+1}$. To deal with this issue, the new system of equations to update the next level of fluid velocity and pressure [11] is presented as follows:

$$\tilde{u}_r^{k+1} = \hat{u}_r^k - \frac{\Delta\tilde{t}}{Re}\frac{\partial\delta}{\partial\tilde{r}}, \quad \tilde{u}_z^{k+1} = \hat{u}_z^k - \frac{\Delta\tilde{t}}{Re}\frac{\partial\delta}{\partial\tilde{z}}, \quad \tilde{p}^{k+1} = \beta\tilde{p}^k + \delta \tag{5}$$

where

$$\hat{u}_r^k = \tilde{u}_r^k + \frac{\Delta\tilde{t}}{Re}\left[-\tilde{u}_r^k\frac{\partial\tilde{u}_r^k}{\partial\tilde{r}} - \tilde{u}_z^k\frac{\partial\tilde{u}_r^k}{\partial\tilde{z}} - \beta\frac{\partial\tilde{p}^k}{\partial\tilde{r}} + \frac{1}{\tilde{r}}\frac{\partial}{\partial\tilde{r}}\left(\tilde{r}\frac{\partial\tilde{u}_r^k}{\partial\tilde{r}}\right) + \frac{\partial^2\tilde{u}_r^k}{\partial\tilde{z}^2} - \frac{\tilde{u}_r^k}{\tilde{r}^2}\right] \tag{6}$$

$$\hat{u}_z^k = \tilde{u}_z^k + \frac{\Delta\tilde{t}}{Re}\left[-\tilde{u}_r^k\frac{\partial\tilde{u}_z^k}{\partial\tilde{r}} - \tilde{u}_z^k\frac{\partial\tilde{u}_z^k}{\partial\tilde{z}} - \beta\frac{\partial\tilde{p}^k}{\partial\tilde{z}} + \frac{1}{\tilde{r}}\frac{\partial}{\partial\tilde{r}}\left(\tilde{r}\frac{\partial\tilde{u}_z^k}{\partial\tilde{r}}\right) + \frac{\partial^2\tilde{u}_z^k}{\partial\tilde{z}^2} - \frac{1}{\tilde{\lambda}_D^2}\tilde{\Psi}\right] \tag{7}$$

The variables $\hat{u}_r^k$ and $\hat{u}_z^k$ are known as the predicted velocities where β is the pressure weight parameter and $\Delta\tilde{t}$ is the time step size. The variable δ in Equation (5) can be obtained by solving the following Poisson's equation:

$$\nabla^2\delta = \frac{1}{\Delta\tilde{t}}\left(\frac{1}{\tilde{r}}\frac{\partial(\tilde{r}\dot{u}_k^r)}{\partial\tilde{r}} + \frac{\partial\dot{u}_z^k}{\partial\tilde{z}}\right). \tag{8}$$

The numerical result is simulated using the Euler forward method with $\Delta\tilde{t} = 1 \times 10^{-5}$ and FDM with 51 and 251 points on r- and z-directions, respectively. The value of δ in Equation (8) is computed using the SOR method for a relaxation parameter $\omega = 1.9$ until the relative error of δ is less than the given SOR tolerance τ.

3. Main Results and Discussions.

3.1. **Fluid phenomena.** The fluid pressure and the fluid velocity in z-direction of the steady state electro-osmotic flow (at time step 10^6) through a cylindrical tube are presented in Figure 2. The velocity in r-direction, which is almost zero in the entire channel, is omitted.

The results in Figure 2(a) show that, the pressure drop decreases in the model with positive value of the external electric field ($\tilde{E} = 1$) compared with the model without the external electric field ($\tilde{E} = 0$). However, the pressure drop increases in the model with negative value of the external electric field ($\tilde{E} = -1$). In addition, the difference of fluid velocity between the channel center and the wall decreases when positive value of $\tilde{E}$ is applied as seen in Figure 2(b). In contrast, the difference of fluid velocity increases when we apply the negative value of $\tilde{E}$.

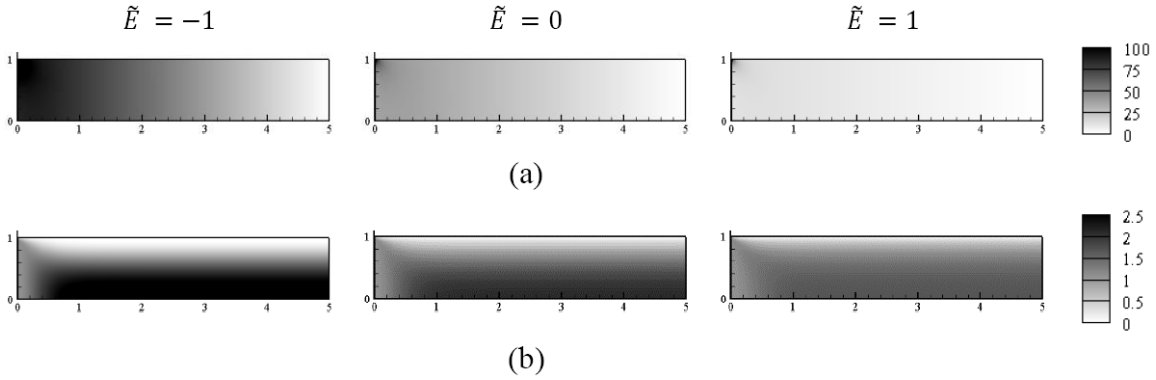

FIGURE 2. (a) Pressure $\tilde{p}$ and (b) z-axis velocity profile $\tilde{u}_z$ of electro-osmotic flow through a cylindrical tube at time step 10^6 with 3 different values of $\tilde{E}$: -1, 0, and 1

Due to the fact that all equations of the SOR method in each time step are the same, the convergent rate of the SOR method can be represented by the number of SOR time steps. Furthermore, to preserve the mass, the fluid velocity should satisfy the continuity equation. However, in a numerical method, the value of the velocity is not equal to zero (we call this as the error of continuity equation). Therefore, in this study, the effect of the pressure weight parameter β, the SOR tolerance τ, and the external electric field $\tilde{E}$ on the convergent rate of the SOR method and the maximum error of the continuity equation are investigated.

3.2. **Effect of the pressure weight parameter β.** Figure 3(a) demonstrates the number of time steps to achieve the SOR method with tolerance $\tau = 10^{-5}$ in each velocity time step starting from 1 to 150000 with 5 different values of β: 0.1, 0.2, 0.4, 0.6, and 0.8. It can be clearly seen that, when β is decreased, the number of SOR time steps decreases even though there is a slightly difference between the models with $\beta = 0.1$ and 0.2. Figure 3(b) presents the maximum error of the continuity equation in each velocity time step starting from 1 to 150000 with 5 different values of β. The figure shows that the maximum error is around 2×10^{-6} in the model with $\beta = 0.1$, and decreases as the value of β is increased.

3.3. **Effect of the SOR tolerance τ.** In Figure 4, using $\beta = 0.1$, we present the effect on the convergent rate of the SOR method and the maximum error of the continuity equation as the tolerance of the SOR method is increased. The result in Figure 4(a)

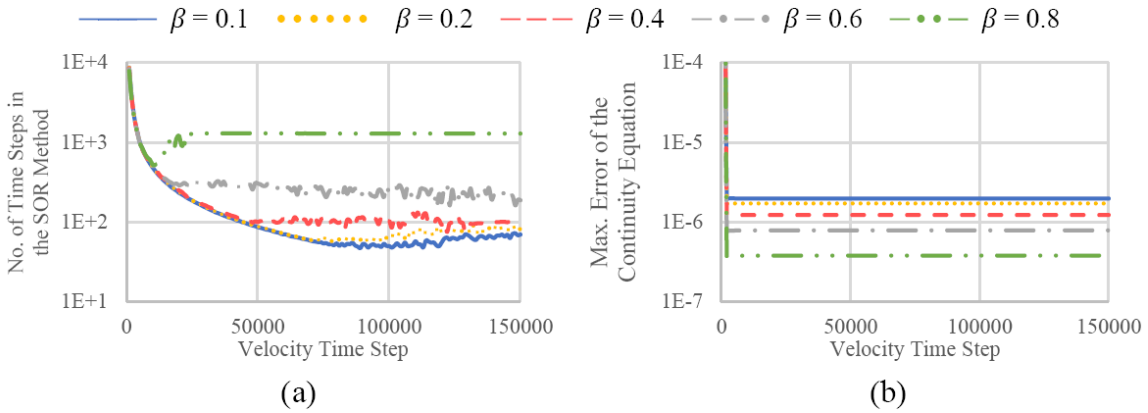

FIGURE 3. (a) The number of SOR time steps and (b) the maximum error of the continuity equation versus velocity time step with 5 different values of β: 0.1, 0.2, 0.4, 0.6, and 0.8

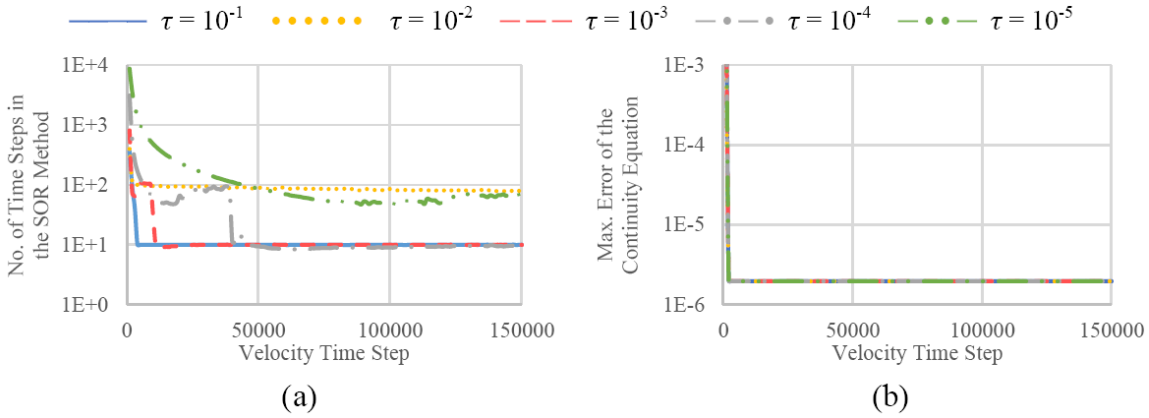

FIGURE 4. (a) The number of SOR time steps and (b) the maximum error of the continuity equation versus velocity time step with 5 different values of τ: 10^{-1}, 10^{-2}, 10^{-3}, 10^{-4} and 10^{-5}

shows that, after velocity time step 50000, the number of SOR time steps reduces from around 60 to around 10 time steps when we increase τ from 10^{-5} to 10^{-3}. But, the number of SOR time steps increases in the model with $\tau = 10^{-2}$ compared with the models with $\tau = 10^{-3}$ and 10^{-4}. However, when we increase the value of τ to 10^{-1}, the number of SOR time steps decreases to around 10 time steps again. Furthermore, when the tolerance is increased to 10^{0}, fluid velocity and pressure diverge at a few hundreds of the velocity time step. Figure 4(b) clearly shows that there is no significant effect on the maximum error of the continuity equation when τ is decreased.

3.4. **Effect of the external electric field $\tilde{E}$.** It is worth mentioning the effect of the external electric field on the convergent rate of the SOR method and the maximum error of the continuity equation as shown in Figure 5 ($\beta = 0.1$ and $\tau = 1 \times 10^{-3}$). In Figure 5(a), It can be found that the number of SOR time steps tends to increase when we apply the external electric field. However, there is no significant effect on the maximum error of the continuity equation when $\tilde{E}$ is decreased as seen in Figure 5(b).

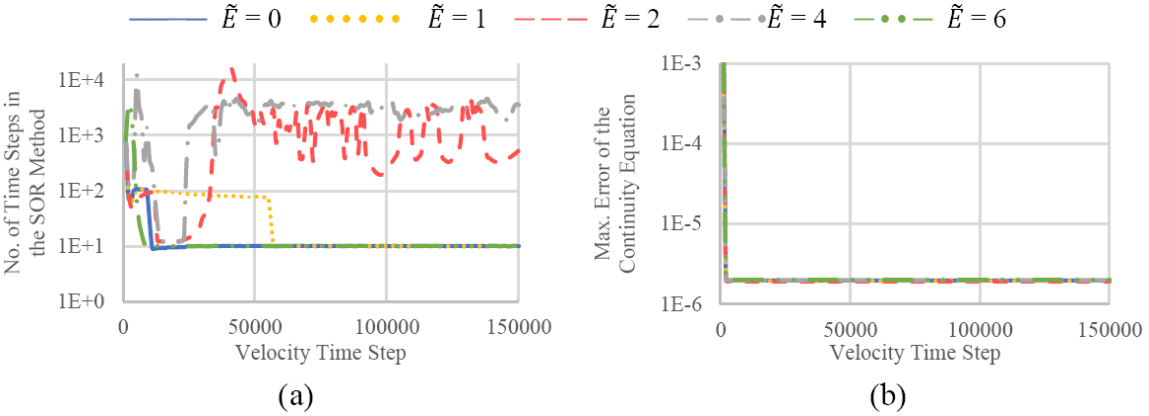

FIGURE 5. (a) The number of SOR time steps and (b) the maximum error of the continuity equation versus velocity time step with 5 different values of $\tilde{E}$: 0, 1, 2, 4, and 6

4. **Conclusions.** We, in this study, aim to present the computational model of electro-osmotic flow through a cylindrical tube and investigate the influence of the pressure weight parameter β, the SOR tolerance τ, and the external electric field $\tilde{E}$ on the convergent rate and the maximum error of the continuity equation. Our results show that one should use

a low-value of β and a high-value of τ to obtain the better computation time. However, too high value of τ can result in the divergence of the velocity value. Moreover, when the electro-osmotic force is applied, the computation time rises up. Therefore, the proper value of the parameters affecting the convergent rate has a high impact on reducing the computation time for the EOF simulation. In future work, we will focus on an application of electro-osmotic forceona control of the concentration gradient of cytokinin which influences the movement of neutrophilin liquid.

Acknowledgment. This work is partially supported by Development and Promotion of Science and Technology Talents Project (DPST) scholarship from Thai government.

REFERENCES

[1] P. Goswami and S. Chakraborty, Semi-analytical solutions for electroosmotic flows with interfacial slip in microchannels of complex cross-sectional shapes, *Microfluid and Nanofluid*, vol.11, pp.255-267, 2011.

[2] R. Ashton, C. Padala and R. S. Kane, Microfluidic separation of DNA, *Current Opinion in Biotechnology*, vol.14, pp.497-504, 2003.

[3] Y. Zhou, A. Deng and C. Wang, Finite-difference model for one-dimensional electro-osmotic consolidation, *Computers and Geotechnics*, vol.54, pp.152-165, 2013.

[4] D. Li, *Electrokinetics in Microfluidics*, Elsevier Academic Press, vol.2, 2004.

[5] M. F. Al-Rjoub, A. K. Roy, S. Ganguli and R. K. Banerjee, Assessment of an active-cooling microchannel heat sink device, using electro-osmotic flow, *International Journal of Heat and Mass Transfer*, vol.54, pp.4560-4569, 2011.

[6] C. Cameselle and K. R. Reddy, Development and enhancement of electro-osmotic flow for the removal of contaminants from soils, *Electrochimica Acta*, vol.86, pp.10-22, 2012.

[7] A. Alizadeh, L. Zhangand and M. Wang, Mixing enhancement of low-Reynolds electro-osmotic flows in microchannels with temperature-patterned walls, *Journal of Colloid and Interface Science*, vol.431, pp.50-63, 2014.

[8] Y. Aboelkassem, Numerical simulation of electroosmotic complex flow patterns in a microchannel, *Computers & Fluids*, vol.52, pp.104-115, 2011.

[9] S. X. Li, Y. J. Jian, Z. Y. Xie, Q. S. Liu and F. Q. Li, Rotating electro-osmotic flow of third grade fluids between two microparallel plates, *Colloids and Surfaces A: Physicochemical and Engineering Aspects*, vol.470, pp.240-247, 2015.

[10] M. Reshadi, M. H. Saidi, B. Firoozabadi and M. S. Saidi, Electrokinetic and aspect ratio effects on secondary flow of viscoelastic fluids in rectangular microchannels, *Microfluid and Nanofluid*, vol.20, 2016.

[11] H. P. Langtangen, K. A. Mardal and R. Winther, Numerical methods for incompressible viscous flow, *Advances in Water Resources*, vol.25, pp.1125-1146, 2002.